Specific heat and phase diagram of heavily doped $La_{1-x}Sr_xMnO_3$ ($0.45 \leqslant x \leqslant 1.0$)

A. Szewczyk,[1,*] M. Gutowska,[1] and B. Dabrowski[2]
[1]*Institute of Physics, Polish Academy of Sciences, Al. Lotników 32/46, 02-668 Warsaw, Poland*
[2]*Department of Physics, Northern Illinois University, DeKalb, Illinois 60115, USA*
(Received 22 August 2005; revised manuscript received 21 October 2005; published 22 December 2005)

Specific heat of stoichiometric $La_{1-x}Sr_xMnO_3$ samples with large ($x=1.0$, 0.9, 0.7, 0.55, 0.45) and low ($x=0.0$) strontium contents was measured from 3 to 393 K, on heating and on cooling, in zero magnetic field and in the field of 7 T. The temperatures and the orders of particular phase transitions have been determined and the poorly known part of the phase diagram, $1 \geqslant x > 0.6$, has been investigated. The phase transitions from the antiferromagnetic ($x=0.0$, 0.7, 1.0) or ferromagnetic ($x=0.45$, 0.55) to the paramagnetic phase were found to be of the second order, when they were purely magnetic transitions, and of the first order, when they were accompanied by the structural transitions, as for example, the transition from the *C*-type antiferromagnetic to the paramagnetic phase coupled with the transformation from the tetragonal to the cubic structure, occurring in the $x=0.9$ composition. The transitions from the *A*- and *C*-type antiferromagnetic phases to the paramagnetic state were influenced stronger by the magnetic field than the transitions from the *G*-type configuration. This behavior was attributed to the presence of ferromagneticaly ordered nearest neighbors within the *A* and *C* configurations and to the presumable quasi one dimensional character of the *C* configuration, indicated also by quantitatively different critical behavior of the specific heat in this phase. The first order transition from the *A*-type antiferromagnetic to the ferromagnetic phase, coupled with the transformation from the tetragonal to the orthorhombic structure, occurring in the $x=0.55$ sample and accompanied by the δ-shaped specific heat anomaly was found to be the most unconventional. It was strongly shifted towards lower temperatures by magnetic field (by ~33 K at 9 T) without substantial change in the shape of the specific heat anomaly. Supplementary magnetization studies revealed the presence of interesting domain structure effects near this transition. By analysis of the temperature dependences of specific heat, two main parameters characterizing the magnetocaloric effect, isothermal change in entropy and adiabatic change in temperature, have been determined. Near the latter transition they reach 3.4 J/(kg K) and −1.5 K, respectively, for the change in magnetic field from 0 to 7 T.

DOI: 10.1103/PhysRevB.72.224429 PACS number(s): 75.40.Cx, 75.30.Kz, 75.30.Sg, 64.70.Kb

I. INTRODUCTION

$La_{1-x}Sr_xMnO_3$ compositions are one of the two most intensively studied series of manganites, because of their intriguing properties such as the colossal magnetoresistance, the strong coupling between magnetic structure and crystal lattice distortions, and the appearance of charge ordering and phase separation over wide ranges of temperature and external magnetic field. Whereas the structure and physical properties of the samples with low strontium content ($x<0.4$) were reported in several hundreds of papers and are rather well known,[1–4] studies of the compositions with higher strontium content ($0.4<x<0.6$) are less frequent[5–10] (around 20 papers), and there are only a few papers[1,11–13] (to the best of our knowledge four) considering properties of the $0.6<x\leqslant 1.0$ samples. This scarcity of data is caused by the inherent difficulty in synthesizing high quality samples of the compositions $0.6<x\leqslant 1.0$, that arises from the small ionic size of the Mn^{4+} ion, i.e., from the unfavorable tolerance factor of the final phase. However, it is important to know the phase diagram for the whole $La_{1-x}Sr_xMnO_3$ system ($0 \leqslant x \leqslant 1.0$). Recently,[11] a two-step method, previously developed for preparation of other metastable compounds,[14,15] has been successfully applied for synthesizing the $La_{1-x}Sr_xMnO_3$ samples with large Sr content ($x>0.45$) and the complete phase diagram of the $La_{1-x}Sr_xMnO_3$ system has been constructed based on the neutron diffraction, resistivity, and magnetic measurements. This diagram, reproduced here in Fig. 1, is similar to the diagram presented in Ref. 12, but it contains additionally the data for the compositional range $0.85<x<1$, which was not considered in Ref. 12 due to the lack of samples. In the diagram, the structural phase transitions that frequently coincide with magnetic transitions, as well as the magnetic transitions occurring between various magnetic phases, i.e., the paramagnetic, the ferromagnetic, and the antiferromagnetic of the *A* type (with ferromagnetic planes ordered antiparallel), the *C* type (with ferromagnetic chains magnetized in opposite directions), and the *G* type (with all magnetic nearest neighbors ordered antiparallel), are denoted by the solid lines.

Since specific heat is the quantity very sensitive to phase transitions of all kinds, its studies are particularly useful for investigations of phase diagrams and often indispensable for unambiguous determination of the orders of considered transitions. Thus, the specific heat measurements of the same $La_{1-x}Sr_xMnO_3$ compositions that were studied in Ref. 11, with $x=1.0$, 0.9, 0.7, 0.55, 0.45, and 0.0, have been performed. Taking into account that the compositions with low strontium content ($0.12 \leqslant x \leqslant 0.2$) were studied in our previous work,[16] particular emphasis was placed on the materials with $x \geqslant 0.45$.

The main purpose of the present work was determining the order of all the observed phase transitions and explaining

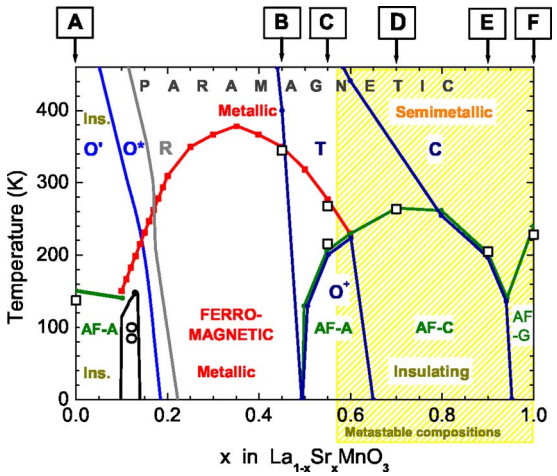

FIG. 1. (Color online) Phase diagram of the $La_{1-x}Sr_xMnO_3$ system for $0 \leqslant x \leqslant 1.0$ (from Ref. 11) with denoted compositions studied in the present work (letters A–F within squares). Open squares denote the points of phase transitions determined from the present specific heat studies. C, T, R, O^*, O', and O^+ denote, respectively, the cubic $Pm\bar{3}m$, tetragonal $I4/mcm$, rhombohedral $R\bar{3}c$, two orthorhombic $Pbnm$, and orthorhombic $Fmmm$ structural phases. AF-A, AF-C, and AF-G stand for the antiferromagnetic phases of the A, C, and G type, respectively. OO denotes the region of stability of the orbitally and charge ordered, insulating, ferromagnetic phase. "Ins." stands for "insulating".

correlations between the shapes of specific heat anomalies accompanying the particular transitions and the magnetic structure of the phases between which the transitions took place. In particular, the anomalies accompanying the phase transitions from the paramagnetic to the antiferromagnetic phase of the A, C, and G type and the transition from the ferromagnetic to the A-type antiferromagnetic phase were thoroughly investigated. Special attention was paid to the transitions from the two different A-type antiferromagnetic phases, i.e., the one occurring in the $x=0$ and the other occurring in the $x=0.55$ sample. The other issue studied was the influence of magnetic field on the phase transitions and on the specific heat anomalies. For the $x=0.55$ sample, additionally the magnetocaloric effect related to this influence, as well as the magnetization have been investigated.

The choice of the particular compositions was based on the following facts. Looking at the phase diagram of the $La_{1-x}Sr_xMnO_3$ system (Fig. 1) we observe the sequential change of the crystalline structure. At room temperature, the heavily doped compounds $(0.75 < x \leqslant 1.0)$ have the cubic $Pm\bar{3}m$ structure of an ideal perovskite. With lowering temperature, the $0.95 < x \leqslant 1.0$ compositions show the magnetic phase transition from the paramagnetic to the G-type antiferromagnetic phase (sample $x=1.0$), whereas the compositions $0.75 < x < 0.95$ display the transition from the paramagnetic to the C-type antiferromagnetic phase, which is the purely magnetic transition for $0.75 < x < 0.8$, and the magnetic transition joined by the structural transformation from the cubic to the tetragonal phase for $0.8 < x < 0.95$. The $x=0.9$ sample was chosen as the representative of the latter range. On decreasing x, the crystalline structure transforms into the tetragonal $I4/mcm$ structure in the result of elongation of the Mn-O6 octahedra along the c axis and their rotation around the c axis (rotation $a^0a^0c^-$, according to the Glazer's notation[17]). At room temperature, this phase is stable for $0.45 < x < 0.75$. On cooling, the compositions from the range $0.6 < x < 0.75$ experience the phase transition from the paramagnetic to the C-type antiferromagnetic phase (the $x=0.7$ sample was the representative of this range), whereas the $0.5 < x < 0.6$ compounds show first the magnetic transition from the paramagnetic to the ferromagnetic phase and next the transition from the ferromagnetic to the A-type antiferromagnetic phase, coupled with the structural transformation from the tetragonal to the orthorhombic $Fmmm$ phase. The low-temperature A-type configuration, consisting of antiferromagnetically coupled ferromagnetic ac planes with the Mn spins pointing along the c axis, is stabilized by the two-dimensional ferromagnetic double exchange interaction, mediated by the $d_{z^2-x^2}$-type orbitals. No canting of the antiferromagnetic sublattices[8–10,18] was evidenced experimentally. Since in this phase some samples exhibit the metallic conductivity and some others exhibit the insulating behavior, there are controversies in literature concerning the conducting properties of this configuration. Some papers state that the two-dimensional band created by the $d_{z^2-x^2}$-type orbitals is responsible for the metallic behavior[9,10,18] of some compositions and the insulating behavior of some polycrystalline samples is caused by the presence of intergrain boundaries. The other papers argue that the A phase is inherently insulating but the phase separation consisting in coexistence of the antiferromagnetic insulating and the ferromagnetic metallic regions is the origin of the metallic behavior observed for some compositions.[7] The $x=0.55$ sample was chosen as the representative of this range. The compositions with $0.45 < x < 0.5$ exhibit on cooling only one magnetic transition from the paramagnetic to the ferromagnetic phase and the $x=0.45$ sample was chosen for the present studies. With further decrease of x, one observes at room temperature the structural transformations from the tetragonal to the rhombohedral $R\bar{3}c$ phase (rotations $a^-a^-a^-$ of the Mn-O6 octahedra), which is stable for $0.17 < x < 0.45$, and then to the two forms of the orthorhombic $Pbnm$ structure (rotations $a^+b^-b^-$) O^* for $0.115 < x < 0.17$ and O' for $0 \leqslant x < 0.115$. As mentioned above, the $0 < x < 0.4$ compositional range was intensively investigated, thus only the $x=0$ sample, in which the purely magnetic transition from the paramagnetic to the A-type antiferromagnetic phase occurs on decreasing temperature, was chosen for the present studies. The A-type configuration occurring in the $x=0.0$ composition has a completely different nature than that observed in the $x \approx 0.55$ samples. This configuration consists of antiferromagnetically coupled ferromagnetic ab planes, with magnetic moments pointing along the orthorhombic b axis. The ferromagnetic ordering within the ab planes is interpreted as the result of the cooperative Jahn-Teller effect, which leads to the appearance of the alternate ordering of orbitals resembling $d_{3x^2-r^2}$ and $d_{3y^2-r^2}$ (the exact shape of these orbitals is still not known), and the presence of the ferromagnetic superexchange interactions between the e_g electrons occupying these orbitals.[19–21] The antiferromagnetic superexchange interactions between t_{2g} elec-

trons are responsible for the antiferromagnetic ordering of the *ab* planes. Moreover, a small canting of the magnetic moments of the antiferromagnetic sublattices due to the antisymmetric Dzialoshinskii-Moriya exchange, absent in the case of the $x \approx 0.55$ compositions, was observed.[22]

II. EXPERIMENT

Polycrystalline samples with $x=0$, 0.45, 0.55, 0.7, 0.9, and 1.0 were prepared using the conventional ceramic method.[23] The stoichiometric $x=0$ sample[24] was obtained in flowing argon at 1400 °C. The $x=0.45$ and 0.55 samples were obtained in air at 1400 °C and then slowly cooled to room temperature. The $x=0.7$, 0.9, and 1.0 samples required the two-step synthesis method.[11] In the first step, single-phase oxygen-deficient perovskites were obtained from precursors fired in flowing argon gas at temperatures up to 1400 °C. In the second step, the oxygen-deficient samples were annealed in air at 500 °C and then slowly cooled to room temperature. The high quality and stoichiometry of these samples were confirmed by x-ray and neutron diffraction studies and thermogravimetric analysis.

Specific heat of all the chosen compositions has been measured over the temperature range from 3 to 393 K on heating, in zero magnetic field B and in the field of 7 T (after cooling the sample in zero magnetic field). For all the samples, measurements on cooling have been performed starting from 393 K down to the temperature lower than the temperature of the lowest lying phase transitions. Data were collected every 0.5 K at low temperatures and in the vicinity of the phase transitions, and every 2 or 5 K outside these regions. It was verified that outside the regions of phase transitions there was no difference between specific heat values measured on heating and on cooling. Additionally, the specific heat of the $x=0$ sample has been measured in $B=9$ T, to investigate the influence of magnetic field on the phase transition from the antiferromagnetic to the paramagnetic phase. For the $x=0.55$ sample, the specific heat measurements in the magnetic field of 1 and 9 T, as well as supplementary magnetization measurements in the field up to 9 T have been performed, in order to investigate the influence of magnetic field on the phase transition from the antiferromagnetic to the ferromagnetic phase. The specific heat was measured by means of the relaxation method, using the heat capacity option of the Physical Properties Measurement System made by Quantum Design. The dc magnetization option of the same system, utilizing the extraction method, was used for the magnetization measurements of the $x=0.55$ sample.

III. RESULTS

The temperature dependences of specific heat measured for all the samples on heating in zero magnetic field are presented in Fig. 2. As indicated in the figure, three kinds of phase transitions were observed in the studied compositions, i.e., the transitions from the ferromagnetic to the paramagnetic phase occurring at the Curie temperature T_C, the transitions from the antiferromagnetic to the paramagnetic phase occurring at the Néel temperature T_N, and the transition from the antiferromagnetic to the ferromagnetic phase at T_{AF-F}. The detailed temperature dependences of specific heat in the vicinity of the phase transitions, measured on heating and on cooling at different values of the magnetic field, are presented in Figs. 3–5. Since the experimental points were measured dense, i.e., every 0.5 K at low temperatures and in the vicinity of the phase transitions, and every 2 or 5 K outside these regions, not all of them are marked with symbols in Figs. 3–5, to avoid overlapping of the symbols and to keep legibility of the graphs.

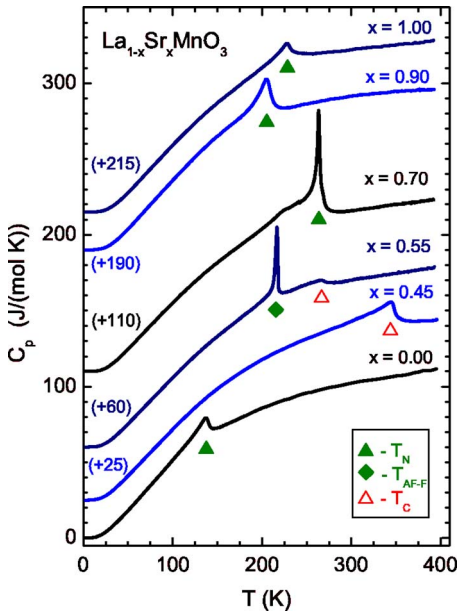

FIG. 2. (Color online) Specific heat of the $La_{1-x}Sr_xMnO_3$ samples measured in zero magnetic field on heating. Numbers in parentheses show the values in J/(mol K) by which the individual curves have been shifted along the C_p axis to avoid overlapping. The symbols indicate the temperatures of phase transitions, i.e., the Curie temperature (open triangles), the Néel temperature (closed triangles) and the temperature of the transition from the ferromagnetic to the antiferromagnetic phase, T_{AF-F} (closed diamond).

Following the analysis presented in our previous paper,[16] the order of each observed phase transition was identified by considering whether the two effects are present, i.e., the hysteresis of appearance of the specific heat anomaly for the measurements performed on heating and on cooling and the difference in the shape of the specific heat anomaly measured on cooling and on heating (the anomaly measured on cooling is usually weaker than that measured on heating). These two effects are the inherent properties of the first order transitions, and they are absent for the second-order transitions.

A. Transition from the ferromagnetic to the paramagnetic phase

The phase transitions from the ferromagnetic to the paramagnetic phase were observed for the $x=0.45$ and 0.55 samples. As shown in Fig. 3, the temperature dependences of specific heat measured on heating and on cooling are indistinguishable, thus these are the second order phase transi-

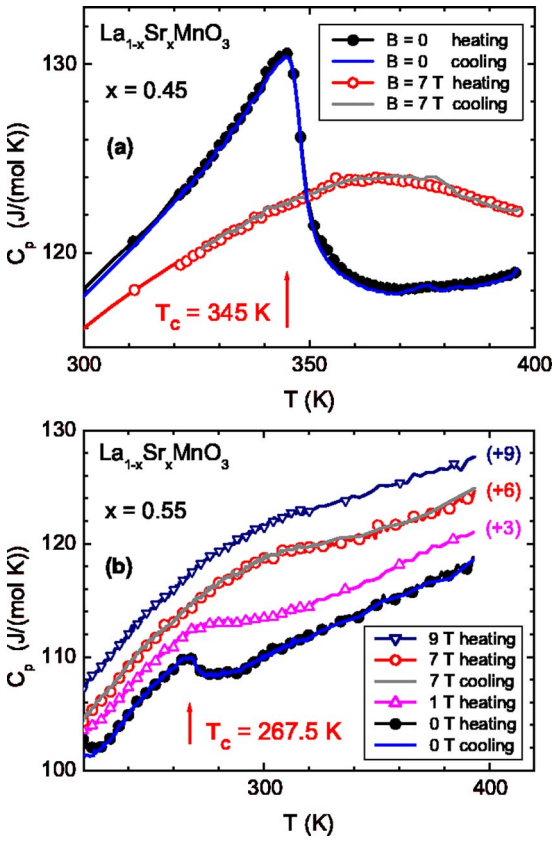

FIG. 3. (Color online) Specific heat anomalies accompanying the second order phase transitions from the ferromagnetic to the paramagnetic phase (at the Curie temperature) in the (a) $x=0.45$ and (b) $x=0.55$ $La_{1-x}Sr_xMnO_3$ compositions. Curves measured on cooling and on heating are indistinguishable. Numbers in parentheses in (b) show values in J/(mol K) by which the individual curves have been shifted along the C_p axis to avoid overlapping.

tions, accompanied by the characteristic λ shaped anomaly. For both compositions, the transitions are purely magnetic (compare Fig. 1), not coupled with any structural transformation, and, as expected, the λ anomaly is shifted to higher temperatures and strongly broadened by the magnetic field.

B. Transition from the antiferromagnetic to the paramagnetic phase

As Fig. 4 illustrates, the specific heat anomalies accompanying the phase transitions from the antiferromagnetic to the paramagnetic phase have diverse shapes and show diverse behavior under influence of the magnetic field depending on the composition and on the type of low-temperature antiferromagnetic configuration. The purely magnetic phase transition from the *G*-type antiferromagnetic structure, occurring in the $x=1.0$ sample [Fig. 4(f)], is of the second order (there is no difference between specific heat measured on heating and on cooling) and it is accompanied by the cusp on the temperature dependence of specific heat. The cusp is insensitive to the magnetic field of 7 T, i.e., it is neither shifted nor broadened, which we attribute to the fact, that in the *G*-type configuration all magnetic nearest neighbors are magnetized antiparallel to each other, so this is the most antiferromagnetic ordering.

The purely magnetic phase transition from the *A*-type antiferromagnetic to the paramagnetic phase, occurring for the other parent compound $x=0.0$ is also visible as the cusp on the temperature dependence of specific heat [Figs. 4(a) and 4(b)]. This is the second order transition, however, contrary to the $x=1.0$ sample, the cusp broadens under influence of the magnetic field [Fig. 4(b)]. There are two origins of this behavior: (1) The magnetic field influences stronger the magnetic structure of the $x=0.0$ sample, because the antiferromagnetic interactions in it are weaker, which is evidenced by the lower value of the Néel temperature. (2) The *A*-type antiferromagnetic ordering, in which each magnetic ion has four in-plane magnetic nearest neighbors aligned ferromagnetically and only two magnetic nearest neighbors magnetized antiparallel, is essentially more susceptible to the magnetic field.

The phase transition from the *C*-type antiferromagnetic to the paramagnetic phase is the most intriguing. In the case of the $x=0.7$ composition [Figs. 4(c) and 4(d)], this is the purely magnetic transition of the second order, accompanied by the narrow and sharp specific heat anomaly qualitatively different from all the other anomalies presented in Figs. 3 and 4. The magnetic field of 7 T shifts the transition towards lower temperatures by around 0.5 K without changing the shape of the specific heat anomaly [Fig. 4(d)]. These facts indicate that the transition belongs to a different universality class than the transitions observed for the $x=1.0$ and $x=0.0$ compositions. This can be attributed to the fact, that the *C*-type configuration consisting of ferromagnetically ordered chains coupled antiferromagnetically, existing within the tetragonal crystal structure, has a definitely anisotropic, uniaxial character, contrary to the *A* and *G* configurations, and that the uniaxial and the isotropic magnetic systems are characterized by the different critical exponents of specific heat α (e.g., $\alpha=-0.08$ for the Heisenberg system and $\alpha=0.119$ for the three-dimensional Ising system). Moreover, the *C*-type magnetic structure of the $x=0.7$ composition can be considered as a quasi-one-dimensional system of ferromagnetically ordered chains weakly coupled antiferromagnetically, i.e., as the system considered theoretically in Ref. 25. Apart from the magnetic anomaly described above, there is a small difference between the temperature dependences of specific heat measured on heating and on cooling below the Néel temperature, around 230 K. It is not related to any phase transition and, at the moment, we have no interpretation of this effect.

In the context of the behavior of the $x=0.7$ sample, it could seem strange that the phase transition from the *C*-type antiferromagnetic to the paramagnetic phase occurring in the $x=0.9$ sample [Fig. 4(e)] is accompanied by the specific heat anomaly of the shape similar to that observed for the $x=1.0$ and 0.0 compositions and that the shape and position of this anomaly are not influenced by the magnetic field of 7 T. However, for the $x=0.9$ compound this is not the purely magnetic transition but the transition coupled with the structural transformation from the tetragonal to the cubic phase. Moreover, the ~0.8 K shift in the cusp position and the difference in the cusp shape for the temperature dependences of

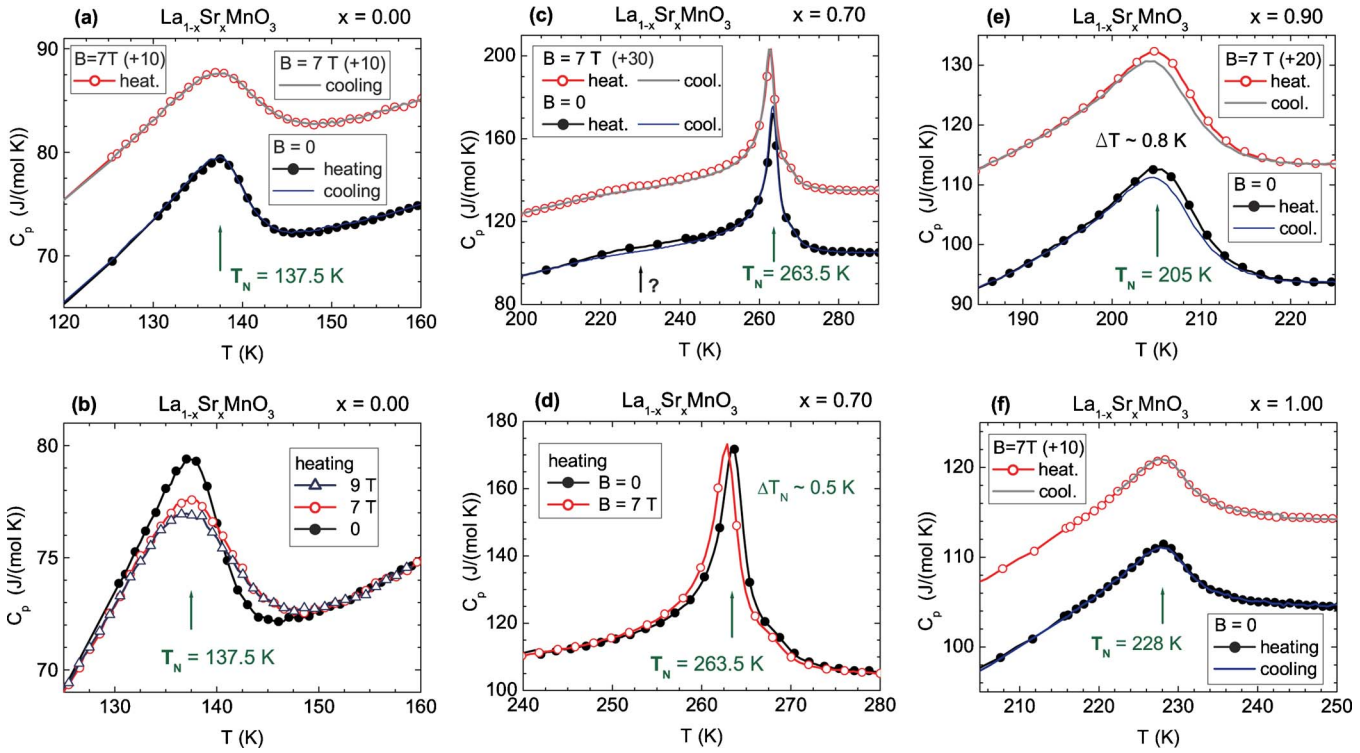

FIG. 4. (Color online) Specific heat anomalies accompanying the phase transitions from the antiferromagnetic to the paramagnetic phase (at the Néel temperature) in the $La_{1-x}Sr_xMnO_3$ compositions. For $x=0.0$ [(a) and (b)], $x=0.7$ [(c) and (d)], and $x=1.0$ (f) these are the second order transitions, whereas for $x=0.9$ (e) this is the first order transition. Curves measured on heating are plotted with solid lines with symbols, curves measured on cooling are plotted with solid lines without symbols. Numbers given in the legends in parentheses show the values in J/(mol K) by which the curves have been shifted along the C_p axis to avoid overlapping. Results measured in the magnetic field of 0, 7, and 9 T are presented.

specific heat measured on heating and on cooling are clearly visible in Fig. 4(e). Thus, this transition was identified as the first order one. In our opinion, the presence of the coupling between the magnetic and the structural transition (essentially not influenced by the magnetic field) changes the order of the phase transition from the second to the first order and makes the transition unaffected by the magnetic field.

C. Transition from the antiferromagnetic to the ferromagnetic phase

The phase transition from the *A*-type antiferromagnetic to the ferromagnetic phase, coupled with the transformation from the orthorhombic to the tetragonal structure, occurring in the $x=0.55$ composition, is the unique one among the studied samples. It is accompanied by the narrow, sharp, δ-shaped specific heat anomaly (Figs. 2 and 5). In Fig. 5, the difference in the position and in the shape of the anomalies registered on heating and on cooling is clearly visible, thus, the transition was identified as the first order one. The external magnetic field shifts strongly the phase transition towards lower temperatures (the field of 9 T lowers the transition temperature by around 33 K) not affecting substantially the shape of the specific heat anomaly and not changing the order of the transition (Fig. 5). Moreover, on the temperature dependences of specific heat there are no indications of the decoupling of the magnetic and the structural transformations. Thus, on the contrary to the transition observed at the Néel temperature for the $x=0.9$ sample, for which the structural transition pins the antiferromagnetic/paramagnetic transition making it insensitive to the magnetic field, the antiferromagnetic/ferromagnetic transition in the $x=0.55$ composition is magnetically driven and the magnetic transition drags the structural transformation along.

Since so strong influence of the magnetic field on the transition without smearing it, seemed to us the very interesting and rare effect, additional studies of the magnetic moment of the sample have been performed. The temperature dependences of magnetization were measured for a series of fixed magnetic field values, from 0 up to 9 T. The magnetic field was applied at low temperature (5 K) after cooling the sample in zero field and then the magnetization was measured on heating up to 320 K and next on cooling down to 5 K. To present the curves measured at the very different magnetic field values in the same graph, the magnetic moment of the sample measured at 240 K for each field value was chosen as the reference value $M_R(T=240\ \mathrm{K}, B=\mathrm{const})$, and the ratio $M(T, B=\mathrm{const})/M_R(T=240\ \mathrm{K}, B=\mathrm{const})$ was plotted in Fig. 6 for all the magnetic field values. To avoid overlapping, the dependences measured at various magnetic field values were shifted along the *y* axis. Figure 6 clearly demonstrates that the magnetic field widens the temperature range of existence of the ferromagnetic phase, without changing the first order character of the antiferromagnet-ferromagnet transi-

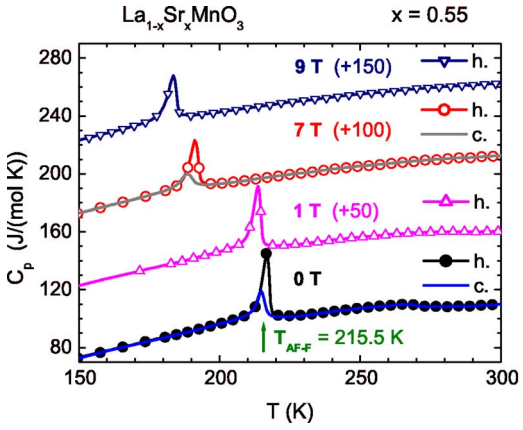

FIG. 5. (Color online) Specific heat anomaly accompanying the first order phase transition from the *A*-type antiferromagnetic to the ferromagnetic phase, coupled with the transformation from the orthorhombic to the tetragonal structure, occurring in the $La_{0.45}Sr_{0.55}MnO_3$ sample. Temperature dependences were measured every 0.5 K in zero magnetic field and in the field of 1, 7, and 9 T. The field of 9 T lowers the phase transition temperature by around 33 K. Curves measured on heating (*h*) are plotted with solid lines with symbols (not all experimental points, measured every 0.5 K, are marked with symbols to keep legibility of the graph), curves measured on cooling (*c*) are plotted with solid lines without symbols. Numbers given above the curves in parentheses are the values in J/(mol K) by which the individual curves have been shifted along the C_p axis to avoid overlapping. The λ anomaly occurring at the Curie temperature, 267.5 K, is hardly noticeable on the scale of the present plot.

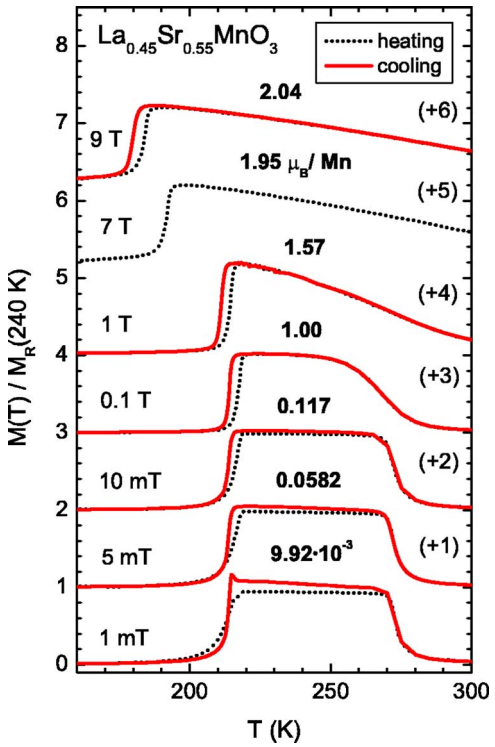

FIG. 6. (Color online) Temperature dependences of the normalized magnetic moment of the $La_{0.45}Sr_{0.55}MnO_3$ sample measured at several fixed values of the magnetic field. The ratio $M(T,B=\text{const})/M_R$ is plotted, where the reference value $M_R(T=240\text{ K}, B=\text{const})$ is the magnetic moment measured at 240 K for each field value. Above each pair of curves (one measured on heating and the other measured on cooling) there are given: the magnetic field value, M_R value (in bold) expressed in μ_B/(Mn ion), and the number in parentheses by which the pair is shifted along the *y* axis to avoid overlapping. On the curve measured in 1 mT on cooling, the characteristic upturn near 215 K, attributed to the domain structure effects, is visible.

tion. The latter observation, which confirms the results of the specific heat studies, follows from the fact that at each field the hysteresis between the dependences measured on heating and on cooling is observed at the shifted transition temperature (with the exception of the case $B=7$ T, for which the measurements were performed on heating only). At the same time, it is clearly visible that the second order ferromagnet-paramagnet transition at the high-temperature side broadens and shifts towards higher temperatures under influence of the magnetic field, in accordance with the results of specific heat studies [Fig. 3(b)].

Taking into account that universality is one of the basic properties of phase transitions and that the typical forms of magnetic domain structure were observed[26] in the $La_{0.875}Sr_{0.125}MnO_3$ manganite, one can assume that the magnetization curves presented in Fig. 6 can be interpreted by using the concepts proposed for other materials showing similar phase transitions,[27] e.g., for $DyFeO_3$, and the theoretical models of domain structure in the vicinity of the Curie temperature.[28] In this context, the narrow temperature range around $T_{AF\text{-}F}$, in which magnetization of the sample rises on heating and falls down on cooling, can be interpreted as the range of appearance of phase domains, i.e., of coexistence of antiferromagnetic and ferromagnetic regions. The latter are divided into magnetic domais[27] in the low fields (up to ~10 mT) and magnetized uniformly in the fields higher than 10 mT. This conclusion is based on the fact that the magnetization values measured at low field (below 10 mT) on cooling are somewhat larger than those measured on heating, which occurs because processes of domain structure nucleation at the first order transition temperature $T_{AF\text{-}F}$ and at the second order transition temperature T_C are entirely different and the evolution of the domain structure is retarded with respect to the temperature changes due to the coercivity. A particularly interesting effect was observed around 3 K above $T_{AF\text{-}F}$ for the sample cooled in the field lower than 5 mT. Then, a well defined cusp appeared on the temperature dependence of magnetization (Fig. 6). As shown in several theoretical papers,[28] in the vicinity of the phase transition the domain walls become wider, which results in decrease of coercivity and in rearrangement of the domain structure. This leads to the increase of the net magnetic moment of the sample and to the appearance of the cusp. We presume that the analogical effect is responsible also for the cusp found for the $Pr_{0.74}Sr_{0.26}MnO_3$ crystal[29] near the temperature of the first order transition from the ferromagnetic to the paramagnetic phase (Fig. 2 of Ref. 29).

D. Magnetocaloric effect related to the antiferromagnet-ferromagnet transition

Over the last several years very intensive search of materials showing large magnetocaloric effect, suitable for appli-

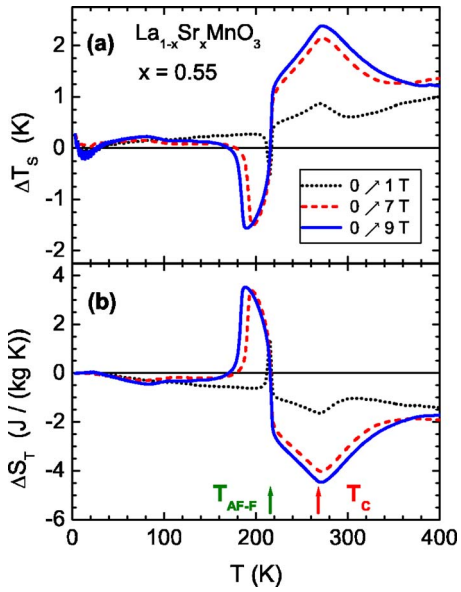

FIG. 7. (Color online) Magnetocaloric effect in the $La_{0.45}Sr_{0.55}MnO_3$ composition. (a) Adiabatic changes in temperature ΔT_S and (b) isothermal changes in entropy ΔS_T resulting from the changes in magnetic field from 0 to 1, 7, and 9 T are plotted as functions of temperature. Both parameters were determined from the temperature dependences of specific heat measured on heating.

cation for magnetic refrigeration, which is thought to be an environmentally friendly technology, eliminating the use of ozone depleting gases, has been performed.[30] As a rule, the magnetocaloric effect is the largest at temperatures of phase transitions at which the magnetization of material changes rapidly.[31,32] Thus, the occurrence of the large magnetocaloric effect in the $La_{0.45}Sr_{0.55}MnO_3$ composition, in the vicinity of the unconventional phase transition from the antiferromagnetic to the ferromagnetic phase strongly affected by the magnetic field, could be expected. To check the validity of this expectation, two basic parameters characterizing the value of magnetocaloric effect, i.e., the adiabatic change in temperature $(\Delta T)_S$ and the isothermal change in entropy $(\Delta S)_T$ induced by the change in magnetic field B, have been determined. By using the measured temperature dependences of specific heat $C(T,B=\text{const})$, the temperature dependences of entropy $S(T,B=\text{const})=\int_0^T[C(T',B)/T']dT'$ were calculated. Next, $(\Delta S)_T$ was determined as $(\Delta S)_T=S(T,B)-S(T,B=0)$, and $(\Delta T)_S$ was determined by solving the equation $S(T+\Delta T,B)=S(T,B=0)$. The results are presented in Fig. 7. Near $T_{\text{AF-F}}$ both parameters reach the values close to those found for other manganites,[30,16,33] i.e., $(\Delta S)_T \approx 3.4$ J/(kg K) and $(\Delta T)_S \approx -1.5$ K for the change of magnetic field from 0 to 7 T. These values are reasonably high but not outstanding in comparison with gadolinium and Gd-based alloys.[30]

IV. CONCLUSIONS

As the result of the performed specific heat measurements, the temperatures of the particular phase transitions occurring in the $La_{1-x}Sr_xMnO_3$ system, as well as their orders have been determined. The phase diagram constructed in Ref. 11 has been confirmed and supplemented. The magnetic phase transitions from the antiferromagnetic and from the ferromagnetic to the paramagnetic phase were found to be of the second order when they were purely magnetic ones. It was found that the kind of critical behavior of the specific heat near the transition from the antiferromagnetic to the paramagnetic phase as well as the influence of the magnetic field on the transition were different for the different antiferromagnetic configurations. This was particularly evident for the quasi-one-dimensional C-type structure present in the $x=0.7$ composition. The magnetic transitions coupled with the structural transformations were found to be of the first order.

The first order phase transition from the A-type antiferromagnetic to the ferromagnetic phase occurring in the $x=0.55$ composition was found to be the most unconventional. The external magnetic field shifts this transition strongly towards lower temperatures (by around 33 K for the field of 9 T) not affecting substantially the shape of the specific heat anomaly (Fig. 5) and not changing the order of the transition. The supplementary magnetization measurements (Fig. 6) revealed the presence of the domain structure effects (in the field lower than 10 mT), among which the appearance of the cusp on the temperature dependence of magnetization measured on cooling in the field of 1 mT was the most interesting. The parameters characterizing magnetocaloric effect (the adiabatic change in temperature and the isothermal change in entropy induced by the change in external magnetic field) related to the first-order antiferromagnet-ferromagnet transition in $La_{0.45}Sr_{0.55}MnO_3$, determined by analyzing the measured temperature dependences of specific heat, were found to be quite large but not outstanding in comparison with other materials considered for application for magnetic refrigeration.

ACKNOWLEDGMENTS

This work was supported in part from the Polish budget founds for scientific research projects for the year 2005. Work at NIU was supported by the NSF Grant No. DMR-0302617.

*Corresponding author. Electronic address: szewc@ifpan.edu.pl

[1] J. B. Goodenough, in *Handbook on the Physics and Chemistry of Rare Earths*, edited by K. A. Gschneidner, Jr., J.-C. G. Bunzli, and V. K. Pecharsky (Elsevier Science, Amsterdam, 2003), Vol. 33, Chap. 214, pp. 249–351.

[2] E. Dagotto, T. Hotta, and A. Moreo, Phys. Rep. **344**, 1 (2001).

[3] *Colossal Magnetoresistance, Charge Ordering and Related Properties of Manganese Oxides*, edited by C. N. R. Rao and B. Raveau (World Scientific, Singapore, 1998).

[4] J. M. D. Coey, M. Viret, and S. von Molnar, Adv. Phys. **48**, 167

(1999).
[5] A. Urushibara, Y. Moritomo, T. Arima, A. Asamitsu, G. Kido, and Y. Tokura, Phys. Rev. B **51**, 14103 (1995).
[6] H. Fujishiro, M. Ikebe, and Y. Konno, J. Phys. Soc. Jpn. **67**, 1799 (1998).
[7] S. I. Patil, S. M. Bhagat, Q. Q. Shu, S. E. Lofland, S. B. Ogale, V. N. Smolyaninova, X. Zhang, B. S. Palmer, R. Decca, F. A. Brown, H. D. Drew, R. L. Greene, I. O. Troyanchuk, and W. H. McCarroll, Phys. Rev. B **62**, 9548 (2000).
[8] J. Dho, W. S. Kim, and N. H. Hur, Phys. Rev. Lett. **87**, 187201 (2001).
[9] Y. Moritomo, T. Akimoto, A. Nakamura, K. Ohoyama, and M. Ohashi, Phys. Rev. B **58**, 5544 (1998).
[10] T. Akimoto, Y. Maruyama, Y. Moritomo, A. Nakamura, K. Hirota, K. Ohoyama, and M. Ohashi, Phys. Rev. B **57**, R5594 (1998).
[11] O. Chmaissem, B. Dabrowski, S. Kolesnik, J. Mais, J. D. Jorgensen, and S. Short, Phys. Rev. B **67**, 094431 (2003).
[12] J. Hemberger, A. Krimmel, T. Kurz, H.-A. Krug von Nidda, V. Yu. Ivanov, A. A. Mukhin, A. M. Balbashov, and A. Loidl, Phys. Rev. B **66**, 094410 (2002).
[13] K. Kikuchi, H. Chiba, M. Kikuchi, and Y. Syono, J. Solid State Chem. **146**, 1 (1999).
[14] D. G. Hinks, B. Dabrowski, J. D. Jorgensen, A. W. Mitchell, D. R. Richards, S. Pei, and D.-L. Shi, Nature (London) **333**, 836 (1988).
[15] B. Dabrowski, O. Chmaissem, J. Mais, S. Kolesnik, J. D. Jorgensen, and S. Short, J. Solid State Chem. **170**, 154 (2003).
[16] A. Szewczyk, M. Gutowska, B. Dabrowski, T. Plackowski, N. P. Danilova, and Yu. P. Gaidukov, Phys. Rev. B **71**, 224432 (2005).
[17] A. M. Glazer, Acta Crystallogr., Sect. B: Struct. Crystallogr. Cryst. Chem. **28**, 3384 (1972).
[18] R. Maezono, S. Ishihara, and N. Nagaosa, Phys. Rev. B **58**, 11583 (1998).
[19] Y. Murakami, J. P. Hill, D. Gibbs, M. Blume, I. Koyama, M. Tanaka, H. Kawata, T. Arima, Y. Tokura, K. Hirota, and Y. Endoh, Phys. Rev. Lett. **81**, 582 (1998).
[20] J. Geck, P. Wochner, S. Kiele, R. Klingeler, A. Revcolevschi, M. v. Zimmermann, B. Büchner, and P. Reutler, New J. Phys. **6**, 152 (2004).
[21] M. Daghofer, A. M. Oles, and W. von der Linden, Phys. Rev. B **70**, 184430 (2004).
[22] G. Matsumoto, J. Phys. Soc. Jpn. **29**, 606 (1970).
[23] B. Dabrowski, X. Xiong, Z. Bukowski, R. Dybzinski, P. W. Klamut, J. E. Siewenie, O. Chmaissem, J. Shaffer, C. W. Kimball, J. D. Jorgensen, and S. Short, Phys. Rev. B **60**, 7006 (1999).
[24] B. Dabrowski, S. Kolesnik, A. Baszczuk, O. Chmaissem, T. Maxwell, and J. Mais, J. Solid State Chem. **178**, 629 (2005).
[25] J. Sznajd, Phys. Rev. B **65**, 224429 (2002).
[26] S. Mori, T. Asaka, Y. Horibe, Y. Matsui, R. Shiozaki, K. Takenaka, and S. Sugai, Mater. Trans., JIM **44**, 2567 (2003).
[27] S. L. Gnatchenko, N. F. Kharchenko, P. P. Lebedev, K. Piotrowski, H. Szymczak, and R. Szymczak, J. Magn. Magn. Mater. **81**, 125 (1989); K. Piotrowski, A. Szewczyk, R. Szymczak, V. V. Eremenko, S. L. Gnatchenko, and N. F. Kharchenko, Acta Phys. Pol. A **68**, 139 (1985); A. Maziewski and R. Szymczak, J. Phys. D **10**, L37 (1977).
[28] V. V. Tarasenko, Fiz. Tverd. Tela (S.-Peterburg) **22**, 503 (1980); V. V. Tarasenko, E. V. Chensky, and I. E. Dikshtein, *ibid.* **18**, 1576 (1976).
[29] V. Markovich, I. Fita, R. Puzniak, A. Wisniewski, K. Suzuki, J. W. Cochrane, Y. Yuzhelevskii, Ya. M. Mukovskii, and G. Gorodetsky, Phys. Rev. B **71**, 224409 (2005).
[30] K. A. Gschneidner, Jr., V. K. Pecharsky, and A. O. Tsokol, Rep. Prog. Phys. **68**, 1479 (2005).
[31] V. V. Khovailo, K. Oikawa, T. Abe, and T. Takagi, J. Appl. Phys. **93**, 8483 (2003); L. Pareti, M. Solzi, F. Albertini, and A. Paoluzi, Eur. Phys. J. B **32**, 303 (2003).
[32] R. Burriel, L. Tocado, E. Palacios, T. Tohei, and H. Wada, J. Magn. Magn. Mater. **290-291**, 715 (2005).
[33] A. Szewczyk, M. Gutowska, K. Piotrowski, and B. Dabrowski, J. Appl. Phys. **94**, 1873 (2003); A. Szewczyk, H. Szymczak, A. Wisniewski, K. Piotrowski, R. Kartaszynski, B. Dabrowski, S. Kolesnik, and Z. Bukowski, Appl. Phys. Lett. **77**, 1026 (2000).